State-observers for differential flatness model based-control of high-performance DC servomotor drives

Yodwong, B.; Thounthong, P.; Sikkabut, S.; Mungporn, P.; Pukdeboon, C.; Sitthithakerngkiet, K.; Kumam, P.; Tricoli, Pietro; Nahid-Mobarakeh, B.; Pierfederici, S.

State-Observers for Differential Flatness Model Based-Control of High-Performance DC Servomotor Drives

B. Yodwong[1,3], P. Thounthong[1,2*], S. Sikkabut[1,3], P. Mungporn[1,3], C. Pukdeboon[4], K. Sitthithakerngkiet[4], P. Kumam[5], P. Tricoli[6], B. Nahid-Mobarakeh[7], and S. Pierfederici[7]

[1]Renewable Energy Research Centre, King Mongkut's University of Technology North Bangkok (KMUTNB), Thailand
[2]Department of Teacher Training in Electrical Engineering, Faculty of Technical Education, KMUTNB, Bangkok, Thailand
[3]Thai-French Innovation Institute, King Mongkut's University of Technology North Bangkok, Bangkok, Thailand
[4]Department of Mathematics, King Mongkut's University of Technology North Bangkok, Bangkok, Thailand
[5]Department of Mathematics, King Mongkut's University of Technology Thonburi, Bangkok, Thailand
[6]School of Electronic, Electrical and Computer Engineering, University of Birmingham, Birmingham, United Kingdom
[7]Groupe de Recherche en Electrotechnique et Electronique de Nancy, Université de Lorraine, Lorraine, France
*e-mail: phtt@kmutnb.ac.th

***Abstract*--Recently, the model based control has been successful applied for motion control applications. It improves better performance than a classic linear control. However, a model base control needs to know some parameters for exact estimations, here a load torque and stator resistance. In this paper, it presents three-observers for a differential flatness model based control approach for a DC permanent magnet motor drive. Observer I is based on the well-known Luenberger estimation (linear approach); Observer II is based on the non-linear approach which guarantees the asymptotical stability; and Obserser III is also based on the non-linear approach which guarantees the exponential stability. To validate the proposed methods, a prototype DC servomotor drive (GEC Alsthom: 2-kW, 2400 rpm) is realized in the laboratory. Simulation and experimental results demonstrate system performance.**

Index Terms-- Flatness control, dc servomtor, Lyapunov function, pulse width modulation, speed control, observer.

I. INTRODUCTION

For more than 50 years, one of the most conventional controller designs for industrial electric motor drives consists of proportional-integral (PI) controllers in a cascade speed/current configuration. The inner-loop controller regulates the motor current (or torque) by providing the reference duty cycle d for power electronic converter (dc/dc or dc/ac), and its external-loop counterpart controls the speed by providing the reference current for the inner loop [1].

However, there are still some aspects of control methods to be studied, particularly in the area of dynamics, robustness, stability, and efficiency. Design controller parameters based on linear methods require a linear approximation, where this is dependent on the operating point. Because the switching model of the dc/dc or dc/ac converter is nonlinear, it is natural to apply model-based nonlinear control strategies that directly compensate for system nonlinearity without requiring a linear approximation [2].

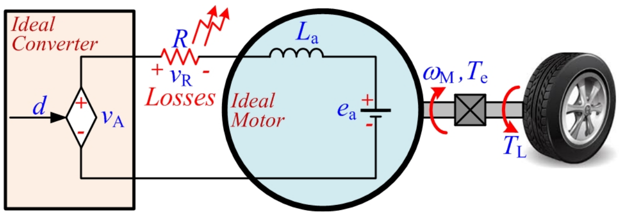

Fig. 1. An equivalent circuit of DC Servomotor drive.

Differential flatness theory (nonlinear approach) was first introduced by Fliess *et al.* [3]. This allowed an alternate representation of the system, where trajectory planning and nonlinear controller design is clear-cut. These ideas have been used lately in a variety of nonlinear power electronic systems [4], [5].

The paper is organized as follows. In section II the equations describing the dc servo drive model are reviewed. Differential flatness based speed/torque feedback control applied to dc servomotor is obtained. The three observers used to servomotor's states and unknown load torque is briefly. System performance is evaluated in section III. Finally, conclusions are drawn in section IV.

II. MODELING, CONTROL, AND OBSERVER

A. Mathematical Model of the DC Servomotor/Converter

The pulse-width modulation PWM technique is applied to a 4-quadrant converter in order to achieve a dc output voltage with a minimum of undesired harmonics. The equipvalent circuit of a dc servo drive is shown in Fig. 1 and the differential equations of motor/converter

This work was supported in part by a research program in cooperation with the Thai-French Innovation Institute, King Mongkut's University of Technology North Bangkok (Thailand), with the Université de Lorraine (France) under Contract KMUTNB–GOV–58–07.

can be written as [1]:

$$\frac{di_a}{dt} = \frac{1}{L}\left(v_a - R \cdot i_a + e_a\right) \quad (1)$$

$$\frac{d\omega_m}{dt} = \frac{1}{J}\left(T_e - B \cdot \omega_m - T_L\right) \quad (2)$$

with,

$$e_a = K_E \cdot \omega_m \quad (3)$$

$$T_e = K_T \cdot i_a \quad (4)$$

where, i_a the armature motor current (A); ω_m the mechanical angular frequency (rad·s^{-1}); L the motor inductance (H); T_e the electromagnetic torque (or motor torque, Nm); T_L the load torque (Nm); K_E the back EMF constant (V·s^{-1}/rad); K_T the torque constant (Nm/A); It should be noted here that a DC motor is always driven by a 4-quadrant dc/dc converter; for this reason, R is simplified as losses in a converter (static and dynamics losses; switching deadtime; voltage drops in IGBTs and Diodes) and in a motor (the stator winding resistance, hysteresis losses, and eddy current losses).

B. Current Control Loop

To prove that the system is flat [5], [6], one defines the flat output y_1, control variable u_1, and state variable x_1 as follows:

$$y_1 = i_a\,,\; u_1 = v_a\,,\; x_1 = i_a \quad (5)$$

Then, the state variables of **x** can be written as

$$x_1 = \varphi_1(y_1) \quad (6)$$

From (1) and (3), the control variable of **u** can be calculated from the flat output **y** and its time derivative (inverse dynamics [6]):

$$\begin{aligned} u_1 &= L \cdot \dot{i}_a + R \cdot i_a - K_E \cdot \omega_m = \psi_1(y_1, \dot{y}_1) \\ &= v_{aREF} \end{aligned} \quad (7)$$

Desired reference for the armature current is represented by y_{1REF} (= i_{aREF}). Feedback control law achieving an exponential tracking of the set-point is given by the following expression [6]:

$$\left(\dot{y}_1 - \dot{y}_{1REF}\right) + K_{11}\left(y_1 - y_{1REF}\right) + K_{12}\int_0^t \left(y_1 - y_{1REF}\right)d\tau = 0 \quad (8)$$

where K_{11} and K_{12} are the controller parameters. One may set the following as a desired characteristic polynomial:

$$p(s) = s^2 + 2\zeta_1\omega_{n1}s + \omega_{n1}^2\,; \quad (9)$$

$$K_{11} = 2\zeta_1\omega_{n1} \quad ;\; K_{12} = \omega_{n1}^2 \quad (10)$$

where ζ_1 and ω_{n1} are the desired dominant damping ratio and natural frequency and new variables are defined $\lambda_1 = \dot{y}_1$.

Trajectory planning is an important step in the implementation of a flatness-based control. It is thus noteworthy to give a well-known waveform such that all the transient state behaviors can be predicted. Next, to limit the transient current, a second order filter is used such that the current command i_{aCOM} is always limited by

$$\frac{i_{aREF}(s)}{i_{aCOM}(s)} = \frac{1}{\left(\frac{s}{\omega_{n2}}\right)^2 + \frac{2\zeta_2}{\omega_{n2}}s + 1} \quad (11)$$

where ζ_2 and ω_{n2} are the desired dominant damping ratio and natural frequency.

C. Speed Control Loop

The outer loop concerns the speed regulation where the flat output y_2, a control variable u_2, and a state variable x_2 are defined:

$$y_2 = \omega_m\,,\; u_2 = i_a\,,\; x_2 = \omega_m \quad (12)$$

So, the flatness based speed controller output generates the command of the armature current, i_{aCOM}. According to mechanical equation (2), and on the assumption that i_a = i_{aCOM} = i_{aREF} because the inner current loop bandwidth is estimated to be faster than the bandwidth of the external speed loop, control variable u_2 (=i_{aCOM}) can be expressed in an *inverse dynamics term* as:

$$\begin{aligned} u_2 &= \left(J \cdot \dot{\omega}_m + T_L - B \cdot \omega_m\right)/K_T = \psi_2(y_2, \dot{y}_2) \\ &= i_{aCOM} \end{aligned} \quad (13)$$

It is similar to the inner current control loop. A desired reference for the mechanical speed is represented by y_{2REF} (= ω_{mREF}). A feedback control law is given by the following expression:

$$\lambda_2 = \dot{y}_{2REF} + K_{21}\left(y_{2REF} - y_2\right) + K_{22}\int_0^t \left(y_{2REF} - y_2\right)d\tau \quad (14)$$

where $K_{21} = 2\zeta_3\omega_{n3}$ and $K_{22} = \omega_{n3}^2$. (15)

Finally, in view of the nature of the derived feedback control law (14) , we need to generate the current command for the converter. Because our focus is on a smooth accelerator or brake (known as a soft-start system), we restrict the reference profiles to smooth changes between stationary regimes. Next, the motion trajectory planning is defined as

$$\frac{\omega_{REF}(s)}{\omega_{COM}(s)} = \frac{1}{\left(\frac{s}{\omega_{n4}}\right)^2 + \frac{2\zeta_4}{\omega_{n4}}s + 1} \quad (16)$$

D. State-Observer

The nonlinear flatness-based control is a model-based control approach. It requires to know system parameters (such stator resistance R, load torque T_L etc.) to obtain the differential flatness property [refer to the dynamics terms (7), (13)]. Then, the online state observers (or parameter observers) are essential to improve the system performance [7].

Refer to (1) – (4), one may write again:

$$\frac{di_a}{dt} = \frac{1}{L}\left(v_a - v_R + K_E \cdot \omega_m\right) \quad (17)$$

$$\frac{d\omega_m}{dt} = \frac{1}{J}\left(K_T \cdot i_a - T_d\right) \quad (18)$$

with

$$v_R = R \cdot i_a \quad (19)$$

$$T_d = B \cdot \omega_m + T_L \quad (20)$$

where v_R represents total losses voltage in the motor and converter [V] and T_d is named here the equivalent load torque [Nm].

In this section, three state observers are proposed. For the first one, it is based on a classic linear Luenberger observer. For the second and the third observers, they are new proposed nonlinear observers. They are dedicated to a specific subclass of nonlinear systems, so one may write as [7]:

$$\begin{cases} \dot{\mathbf{X}} = \begin{pmatrix} \dot{\mathbf{x}} \\ \dot{\mathbf{p}} \end{pmatrix} = \begin{pmatrix} f(x,u) + g(x,u) \cdot \mathbf{p} \\ 0 \end{pmatrix} \\ \mathbf{Y} = \mathbf{x} \end{cases} \quad (21)$$

where:

1) X $\in \Re^{n\times m}$ is the vector of variable which is going to be estimated, and Y $\in \Re^{n}$ is the vector of measured variables;

2) $\mathbf{x} \in \Re^{n}$ is the vector of the system state variables. Every state variable is supposed to be measured (i.e., $\mathbf{Y} = \mathbf{x}$);

3) $\mathbf{p} \in \Re^{m}$ is the vector of the unknown parameters to estimate. Parameters $\mathbf{p}$ are supposed to vary slowly compared to state variables $\mathbf{x}$;

4) f and g are nonlinear functions of $\mathbf{x}$ and $\mathbf{u}$ (the command signal vector), respectively, of size $\Re^{n}$ and $\Re^{n\times m}$.

Refer to (17) and (18), one defines:

$$\mathbf{x} = \begin{bmatrix} x_1 \\ x_2 \end{bmatrix} = \begin{bmatrix} i_a \\ \omega_m \end{bmatrix}, \ \mathbf{p} = \begin{bmatrix} p_1 \\ p_2 \end{bmatrix} = \begin{bmatrix} v_R \\ T_L \end{bmatrix} \quad (22)$$

$$f(x,u) = \begin{bmatrix} \frac{v_a}{L} - \frac{K_E \cdot \omega_m}{L} \\ \frac{K_T \cdot i_a}{J} \end{bmatrix} \quad (23)$$

$$g(x,u) = \begin{bmatrix} \frac{-1}{L} & 0 \\ 0 & \frac{-1}{J} \end{bmatrix} \quad (24)$$

1). Observer I: Luenberger observer

As it a state observer dedicated to linear systems, it is necessary to linearize the considered system around one operating point. The observer is used to estimate the state vector $\mathbf{x}$ of (17) and (18) from knowledge of the input vector $\mathbf{u}$ (= v_a) and direct measurement of the output vector $\mathbf{y}$ and the observer gain matrix $\mathbf{G}$

$$\dot{\hat{\mathbf{x}}} = \mathbf{A}\hat{\mathbf{x}} + \mathbf{B}\mathbf{u} - \mathbf{G}(\hat{\mathbf{y}} - \mathbf{y}) \quad (25)$$

$$\hat{\mathbf{y}} = \mathbf{C}\hat{\mathbf{x}} \quad (26)$$

with

$$\mathbf{A} = \begin{bmatrix} 0 & -\frac{K_E}{L} & -\frac{1}{L} & 0 \\ \frac{K_T}{J} & 0 & 0 & -\frac{1}{J} \\ 0 & 0 & 0 & 0 \\ 0 & 0 & 0 & 0 \end{bmatrix}, \ \mathbf{B} = \begin{bmatrix} \frac{1}{L} \\ 0 \\ 0 \\ 0 \end{bmatrix}$$

$$\mathbf{C} = \begin{bmatrix} 1 & 0 & 0 & 0 \\ 0 & 1 & 0 & 0 \end{bmatrix}, \ \mathbf{x} = \begin{bmatrix} i_a & \omega_m & v_R & T_d \end{bmatrix}^t \quad (27)$$

The observer poles should be selected according to the system requirements, which are typically rapid response and stable and accurate estimation, as shown in the following:

$$\det(\boldsymbol{\lambda}\mathbf{I} - (\mathbf{A} - \mathbf{GC})) = 0. \quad (28)$$

with eigenvalues $\boldsymbol{\lambda}$ with negative real part.

2). Observer II: Asymptotically Stable

For the subclass of nonlinear systems verifying (21), the proposed state observer II is defined, considering the estimation errors $\mathbf{e}_x = (\hat{\mathbf{x}} - \mathbf{x})$ and $\mathbf{e}_p = (\hat{\mathbf{p}} - \mathbf{p})$

$$\begin{pmatrix} \dot{\hat{\mathbf{x}}} \\ \dot{\hat{\mathbf{p}}} \end{pmatrix} = \begin{bmatrix} f(x,u) + g(x,u) \cdot \hat{\mathbf{p}} - \mathbf{S}_1 \cdot \mathbf{e}_x \\ -g^t(x,u) \cdot \mathbf{e}_x \end{bmatrix} \quad (29)$$

with

$\mathbf{S}_1$ is the positive-definite matrix of size $\Re^{n\times n}$.

Proof: the derivative estimation errors $\mathbf{e}_x$ and $\mathbf{e}_p$ are written, respectively, as follows:

$$\dot{\mathbf{e}}_x = g(x,u) \cdot \mathbf{e}_p - \mathbf{S}_1 \cdot \mathbf{e}_x \quad (30)$$

$$\dot{\mathbf{e}}_p = -g^t(x,u) \cdot \mathbf{e}_x \quad (31)$$

Asymptotic stability of this estimation can be demonstrated with the classical Lyapunov approach. The Lyapunov candidate function, V is considered as follows:

$$V = \frac{1}{2}\begin{pmatrix} \mathbf{e}_x & \mathbf{e}_p \end{pmatrix} \cdot \begin{pmatrix} \mathbf{e}_x \\ \mathbf{e}_p \end{pmatrix} \geq 0 \quad (32)$$

The derivative of function V can be expressed as

$$\dot{V} = \mathbf{e}^t{}_x \cdot \dot{\mathbf{e}}_x + \mathbf{e}^t{}_p \cdot \dot{\mathbf{e}}_p \quad (33)$$

By combining (30), (31), and (33), $\dot{V}$ can be expressed as

$$\dot{V} = \mathbf{e}^t{}_x \cdot g(x,u) \cdot \mathbf{e}_p - \mathbf{e}^t{}_x \cdot \mathbf{S}_1 \cdot \mathbf{e}_x + \mathbf{e}^t{}_p \left(-g(x,u) \cdot \mathbf{e}_x\right) \quad (34)$$

Finally,

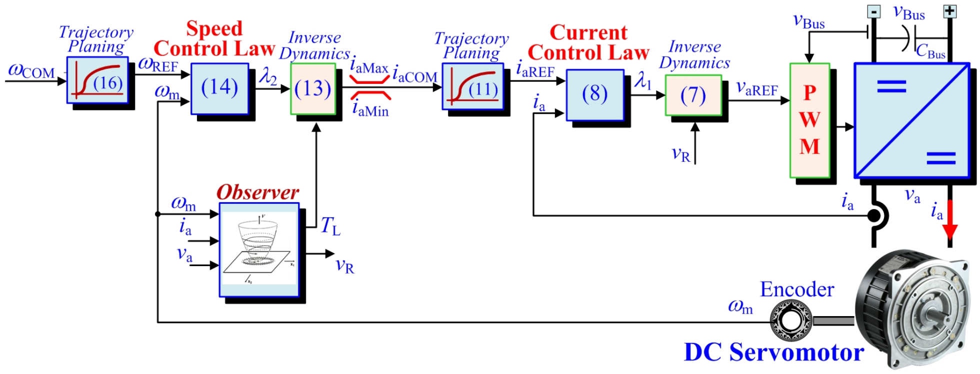

Fig. 2. Proposed a differential flatness based speed/torque control of a dc servomotor drive with state-observer.

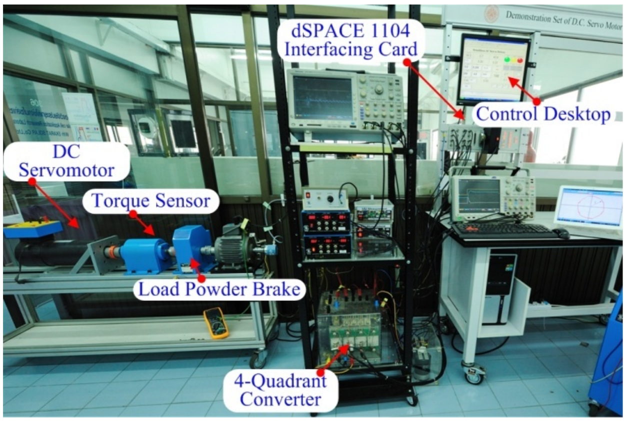

Fig. 3. Test bench of the DC Servomotor drive.

$$\dot{V} = -\mathbf{e}^t{}_{\mathrm{x}} \cdot \mathbf{S}_1 \cdot \mathbf{e}_{\mathrm{x}} < 0 \tag{35}$$

So, the estimation asymptotical stability can be ensured long as $\mathbf{S}_1$ is positive-definite matrix.

2). Observer III: Exponentially Stable

The proposed non-linear state observer III is defined as

$$\begin{pmatrix} \dot{\hat{\mathbf{x}}} \\ \dot{\hat{\mathbf{p}}} \end{pmatrix} = \begin{bmatrix} f(x,u) + g(x,u) \cdot \hat{\mathbf{p}} - \mathbf{S}_2 \cdot \mathbf{e}_{\mathrm{x}} \\ \mathbf{K}_{\mathrm{p}} \cdot \dot{\mathbf{e}}_{\mathrm{x}} + \mathbf{K}_{\mathrm{i}} \cdot \mathbf{e}_{\mathrm{x}} - g^t(x,u) \cdot \mathbf{e}_{\mathrm{x}} \end{bmatrix} \tag{36}$$

with
$\mathbf{S}_2$ is the positive-definite matrix of size $\Re^{n \times n}$.
$\mathbf{P}$ is the positive-definite matrix of size $\Re^{m \times m}$.
and,

$$\mathbf{K}_{\mathrm{p}} = -\mathbf{P} \cdot g^{-1}(x,u) \tag{37}$$

$$\mathbf{K}_{\mathrm{i}} = \mathbf{K}_{\mathrm{p}} \cdot \mathbf{S}_2 \tag{38}$$

Proof: it is similar to the proposed observer II. The derivative of Lyapunov function V can be expressed as

$$\begin{aligned} \dot{V} &= \mathbf{e}^t{}_{\mathrm{x}} \cdot g(x,u) \cdot \mathbf{e}_{\mathrm{p}} - \mathbf{e}^t{}_{\mathrm{x}} \cdot \mathbf{S}_2 \cdot \mathbf{e}_{\mathrm{x}} \\ &+ \mathbf{e}^t{}_{\mathrm{p}} \cdot \mathbf{K}_{\mathrm{p}} \cdot g(x,u) \cdot \mathbf{e}_{\mathrm{p}} - \mathbf{e}^t{}_{\mathrm{p}} \cdot \mathbf{K}_{\mathrm{p}} \cdot \mathbf{S}_2 \cdot \mathbf{e}_{\mathrm{x}} \\ &+ \mathbf{e}^t{}_{\mathrm{p}} \cdot \mathbf{K}_{\mathrm{i}} \cdot \mathbf{e}_{\mathrm{x}} - \mathbf{e}^t{}_{\mathrm{p}} \cdot g^t(x,u) \cdot \mathbf{e}_{\mathrm{x}}. \end{aligned} \tag{39}$$

Then, by introducing $\mathbf{K}_{\mathrm{p}} \cdot g(x, u) = -\mathbf{P}$ and $\mathbf{K}_{\mathrm{i}} = \mathbf{K}_{\mathrm{p}} \cdot \mathbf{S}_2$, it results

Table I. DC servomtor/converter specification and parameters.

Rated Power P_{rated}	2000	W
Rated Speed n_{rated}	2400	rpm
Rated Torque T_{rated}	7.8	Nm
Resistance (Motor+Inverter) R	1.48	Ω
Armature inductance L	2.1	mH
Equivalent inertia J	7.1×10^{-3}	kg· m^2
Viscous friction coefficient B	6.8×10^{-4}	Nm· s/rad
Torque Constant K_{T}	0.4875	Nm/A
V_{Bus}	134	V
V_{aMax}	134	V
Switching Frequency f_{S}	10	kHz

Table II. Speed/current regulation parameters.

ζ_1	1	pu.
ω_{n1}	2500	rad· s^{-1}
ζ_2	1	pu.
ω_{n2}	250	rad· s^{-1}
ζ_3	1	pu.
ω_{n3}	25	rad· s^{-1}
ζ_4	1	pu.
ω_{n4}	25	rad· s^{-1}
i_{aMax}	+20	A
i_{aMin}	−20	A

$$\dot{V} = -\begin{bmatrix} \mathbf{e}_{\mathrm{x}} & \mathbf{e}_{\mathrm{p}} \end{bmatrix} \cdot \begin{bmatrix} \mathbf{S}_2 & 0 \\ 0 & \mathbf{P} \end{bmatrix} \cdot \begin{bmatrix} \mathbf{e}_{\mathrm{x}} \\ \mathbf{e}_{\mathrm{p}} \end{bmatrix} < -\alpha \cdot V < 0\,. \tag{40}$$

where, α is a defined minimum rate of decay. The estimation exponential stability can be ensured long as **S2** and **P** are positive-definite matrix. The tuning of the $\mathbf{S}_2$ and **P** matrices is based on the assumption that the dynamics of the state vector error $\mathbf{e}_{\mathrm{x}}$ have to be highly faster than the dynamics of the parameter vector error $\mathbf{e}_{\mathrm{p}}$. This choice involves a design of the matrix $\mathbf{S}_2$ with eigenvalues real parts highly greater than those of **P**.

E. Control Conclusion

In Fig. 2, the proposed control algorithm, as detailed earlier, is depicted. The external speed control algorithm generates a current command i_{aCOM}. This signal must be saturated within an interval [i_{aMax}, i_{aMin}]. The inner current control algorithm estimates the voltage references. This results in voltage references v_{a}.

Based on the power electronic constant switching frequency ω_{S} and cascade control structure, the outer speed control loop must operate at a cutoff frequency $\omega_{\mathrm{n3}} << \omega_{\mathrm{n2}} << \omega_{\mathrm{n1}} << \omega_{\mathrm{S}}$ [6]. However, to increase the speed respose, one may set $\omega_{\mathrm{n4}} = \omega_{\mathrm{n3}}$. For system damping ratios, one may set $\zeta_4 = \zeta_3 = \zeta_2 = \zeta_1 = 1$ pu. Once the flat outputs are stabilized, the whole system is stable because all the variables of the system are expressed in terms of the flat outputs. The three observers are studied in order to estimate v_R and T_d, so that v_R_I, v_R_II, v_R_III and T_d_I, T_d_II, T_d_III are calculated from the observer I, II, and III, repectively.

III. Performance Validation

In order to authenticate the proposed control algorithm and control laws, a small-scale test bench of the dc servomotor drive was implemented in our laboratory, as presented in Fig. 3. The dc motor used in this effort was a brush dc servomotor (2 kW, 2400 rpm). The motor/converter specification and parameters are presented in Table I used for following simulations and experimentations. The machine parameters were obtained from the *offline identifications*, in which the motor was connected with the 4-quadrant converter. For this reason, the simplified resistance R is quite high, because it represents some losses in the cables, the converter, and motor. Parameters associated with the speed/torque regulation loops can be seen in Table II. Moreover, these control loops, which generated voltage references v_a were implemented in the real-time card dSPACE DS1104 (see Fig. 3) using MATLAB–Simulink.

A. Observers Test

The performance comparisons between a classical linear observer and two nonlinear observers are presented as follows. At first, the observers are used for state-estimation only; for this reason, a classic linear PI based speed/current cascade control is implemented. The matrix observers parameters are as follows:

$$\mathbf{G}=\begin{bmatrix}500.00 & -232.14\\ 68.66 & 150.00\\ -126.00 & 0.00\\ 0.00 & -35.50\end{bmatrix}, \text{ observer I.}$$

$$\mathbf{S}_1=\begin{bmatrix}400.00 & 0.00\\ 0.00 & 400.00\end{bmatrix}, \text{ observer II.}$$

$$\mathbf{S}_2=\begin{bmatrix}700.00 & 0.00\\ 0.00 & 700.00\end{bmatrix}\ \mathbf{P}=\begin{bmatrix}70.00 & 0.00\\ 0.00 & 70.00\end{bmatrix} \text{ observer III.}$$

Figs. 4 and 5 show the experimental results obtained for three observers at different operating points to observe T_d and v_R. In Fig. 4, they show Ch1: n, Ch2: i_a, Ch3: T_e, Ch4: T_d_I, Ch5: T_d_II, and Ch6: T_d_III. In Fig. 5, they show Ch1: n, Ch2: i_a, Ch3: T_e, Ch4: v_R_I, Ch5: v_R_II, and Ch6: v_R_III. The studied estimations are verified to converge to the desired values for each state observers. Also, it can be observed that the Luenberger state observer is slower to converge and the observer III (exponentially stable) is fastest to converge. For this reason, only observer III is selected to realize as a state observer for the flatness based speed/current control of a dc servomotor drive as follows.

B. Speed/Current Control Loop Test

Figs. 6 and 7 show the experimental results obtained for the flatness current control during the current command i_{aCOM} step from 3 A to 6 A and 6 A to 2 A, respectively. They show i_{aCOM}, i_{aREF}, i_a, and the speed n. One may observe that the current i_a follows its reference i_{aREF} perfectly: fast and smooth response.

Finally, Fig. 8 also shows the simulation results by using MATLAB/simulink software obtained for the flatness speed/current control during the T_d step from 1 Nm to 5 Nm at the speed command of 1000 rpm. The flatness-based control with a proposed observer shows good stability and optimum response of the speed regulation to its desired reference. The speed regulation is minimally influenced by the large step in load torque disturbance.

IV. Conclusions

This paper presented a modeling and control for a dc servomotor drive and state–observers dedicated to online estimation. The knowledge of the electric drive system is very useful for designing model-based controls, control schemes, or diagnosis possibilities. The three observers introduced was used to estimate the variables to be fed back to nonlinear controllers. The proposed control scheme was tested by simulations and real experimentations, presenting a very satisfactory performance in the whole speed range, with varying load torque and uncertainties in the mechanical parameters.

Finally, the new proposed control and observer are useful and may apply for other motion control applications such induction motor or PMSM drives.

References

[1] Young Ik Son, In Hyuk Kim, Dae Sik Choi, and Hyungbo Shim, "Robust Cascade Control of Electric Motor Drives Using Dual Reduced-Order PI Observer," *IEEE Trans. Ind. Electron*., vol. 62, no. 6, pp. 3672–3682, June 2015.

[2] P. Thounthong, "Control of a Three-Level Boost Converter Based on a Differential Flatness Approach for Fuel Cell Vehicle Applications," *IEEE Trans. Veh. Technol.*, vol. 61, no. 3, pp. 1467–1472, Mar. 2012.

[3] M. Fliess, J. Levine, P. h. Martin, and P. Rouchon, "A Lie–Bäcklund approach to equivalence and flatness of nonlinear systems," *IEEE Trans. Automat. Contr*., vol. 44, no. 5, pp. 922–937, May 1999.

[4] P. Thounthong, P. Tricoli, and B. Davat, "Performance investigation of linear and nonlinear controls for a fuel cell/supercapacitor hybrid power plant," *Int. J. Elect. Power Energy Syst*., vol. 54, pp. 454–464, Jan. 2014

[5] M. Pahlevaninezhad, P. Das, J. Drobnik, P. K. Jain, and A. Bakhshai, "A New Control Approach Based on the Differential Flatness Theory for an AC/DC Converter Used in Electric Vehicles," *IEEE Trans. Power Electron*., vol. 27, no. 4, pp. 2085–2103, Apr. 2012.

[6] P. Thounthong *et al*., "DC bus stabilization of li-ion battery based energy storage for a hydrogen/solar power plant for autonomous network applications," *IEEE Trans. Ind. Appl*., vol. 51, no. 4, pp. 2717–2725, Jul./Aug. 598 2015.

[7] H. Renaudineau, J.-Ph. Martin, B. Nahid-Mobarakeh, and S. Pierfederici, "DC–DC converters dynamic modeling with state observer-based parameter estimation," *IEEE Trans. Power Electron*., vol. 30, no. 6, pp. 3356–3363, June 2015.

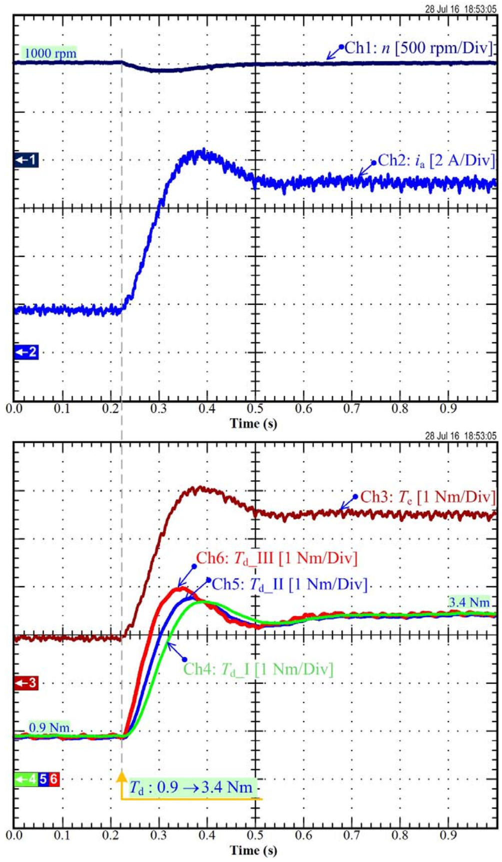

Fig. 4. Experimental result: T_d estimations at n = 1000 rpm and T_d step: 0.9 → 3.4 Nm.

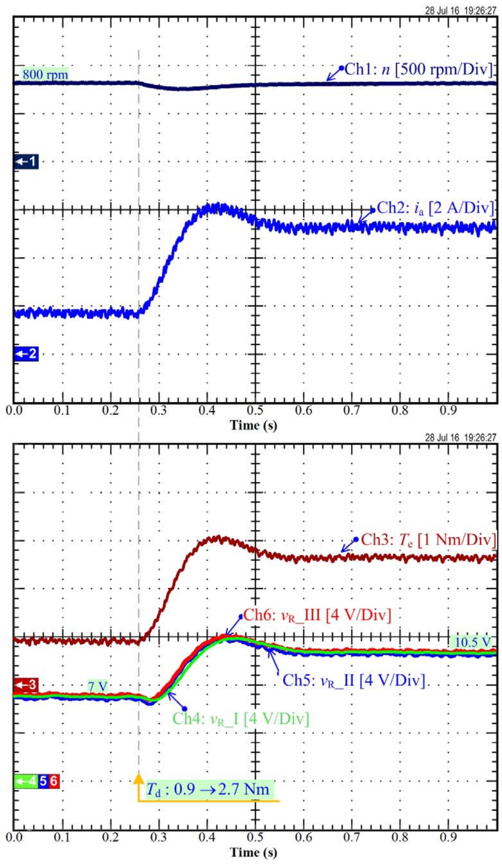

Fig. 5. Experimental result: v_R estimations at n = 800 rpm and T_d step: 0.9→ 2.7 Nm.

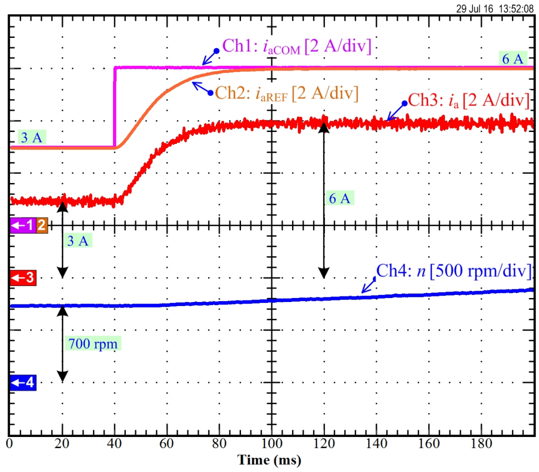

Fig. 6. Experimental result: Flatness based current control at a current i_{aCOM} step from 3 A to 6 A, at an initial speed of 700 rpm.

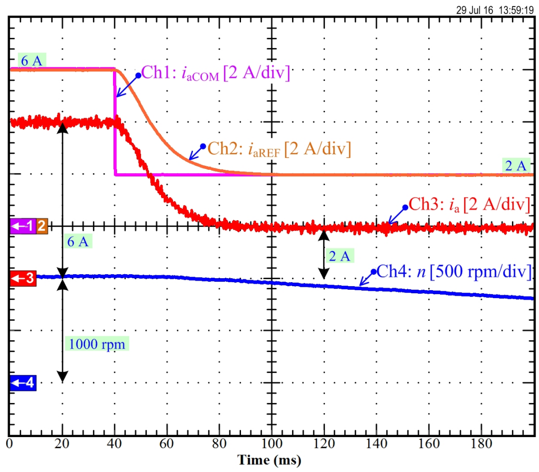

Fig. 7. Experimental result: Flatness based current control at a current i_{aCOM} step from 6 A to 2 A, at an initial speed of 1000 rpm.

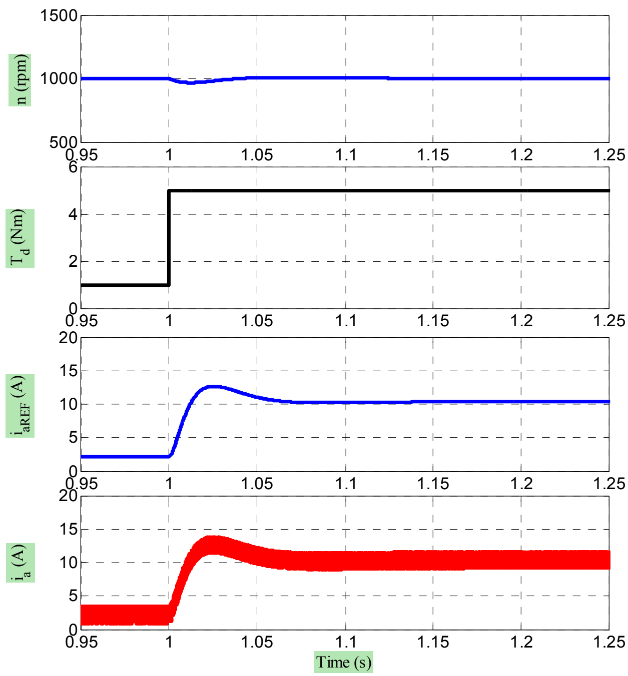

Fig. 8. Simulation results: Flatness based speed/current control at T_d step from 1 Nm to 5 Nm, and n_{COM} = 1000 rpm.